CSIRO PUBLISHING
Exploration Geophysics
http://dx.doi.org/10.1071/EG14121

An efficient hybrid scheme for fast and accurate inversion of airborne transient electromagnetic data

Anders Vest Christiansen[1,4] Esben Auken[1] Casper Kirkegaard[1] Cyril Schamper[2] Giulio Vignoli[3]

[1]Department of Geoscience, Aarhus University, Aarhus 8000, Denmark.
[2]Unité Mixte de Recherche 7619 Sisyphe, Université Pierre et Marie Curie, 75252 Paris, France.
[3]Geological Surveys of Denmark and Greenland, Aarhus 8000, Denmark.
[4]Corresponding author. Email: anders.vest@geo.au.dk

Abstract. Airborne transient electromagnetic (TEM) methods target a range of applications that all rely on analysis of extremely large datasets, but with widely varying requirements with regard to accuracy and computing time. Certain applications have larger intrinsic tolerances with regard to modelling inaccuracy, and there can be varying degrees of tolerance throughout different phases of interpretation. It is thus desirable to be able to tune a custom balance between accuracy and compute time when modelling of airborne datasets. This balance, however, is not necessarily easy to obtain in practice. Typically, a significant reduction in computational time can only be obtained by moving to a much simpler physical description of the system, e.g. by employing a simpler forward model. This will often lead to a significant loss of accuracy, without an indication of computational precision.

We demonstrate a tuneable method for significantly speeding up inversion of airborne TEM data with little to no loss of modelling accuracy. Our approach introduces an approximation only in the calculation of the partial derivatives used for minimising the objective function, rather than in the evaluation of the objective function itself. This methodological difference is important, as it introduces no further approximation in the physical description of the system, but only in the process of iteratively guiding the inversion algorithm towards the solution. By means of a synthetic study, we demonstrate how our new hybrid approach provides inversion speed-up factors ranging from ~3 to 7, depending on the degree of approximation. We conclude that the results are near identical in both model and data space. A field case confirms the conclusions from the synthetic examples: that there is very little difference between the full nonlinear solution and the hybrid versions, whereas an inversion with approximate derivatives and an approximate forward mapping differs significantly from the other results.

Key words: AEM, approximate Jacobian, hybrid minimisation, large dataset inversion.

Received 25 November 2014, accepted 8 July 2015, published online 13 August 2015

Introduction

The airborne transient electromagnetic (TEM) method has its roots in mineral exploration (see Allard (2007) for an overview), but also finds extensive use in modern applications such as geothermal studies (Legault et al., 2011), groundwater investigation (e.g. Siemon et al., 2009; Kirkegaard et al., 2011) and petroleum resource characterisation (Pfaffhuber et al., 2009). Most modern applications require high resolution capabilities and dense data coverage, resulting in surveys that often span thousands of line-kilometres of densely collected sounding data. For the interpretation of such large-scale datasets, it is common to choose a balanced scheme for the modelling, i.e. one that provides the most attractive compromise between precision and computational complexity. In many cases of mineral exploration, it is possible to identify targets by means of direct inspection of the data, making exhaustive modelling unnecessary. For applications that require more quantitative results, fast interpretation tools can be found within the family of conductivity-depth transforms (e.g. Huang and Fraser, 1996; Macnae et al., 1998; Sengpiel and Siemon, 2000; Zhdanov, 2002). Such methods provide means for a direct and extremely fast translation of the measured data into resistivity parameters of interest, having no need for inversion schemes or complex forward modelling of the underlying physical system. This type of approach has proven very successful in the past, but unfortunately it comes without a well defined measure of data fit, and it provides no means for estimating uncertainty either. Thus, for applications that require a high degree of accuracy, the only acceptable solution is provided by inversion in combination with a suitable forward model.

Today, one-dimensional (1D) forward modelling that includes all characteristics of the instrument transfer function is an efficient and popular choice (Auken et al., 2014). Efficient forward models in two-dimensions (2D) (Wilson et al., 2006) and even three-dimensions (3D) (Cox et al., 2010) are also being employed. Ley-Cooper et al. (2015) discuss the choice of 1D versus 2D and 3D in a detailed analysis of an Australian dataset. A similar discussion is found in Viezzoli et al. (2010) and in Minsley et al. (2012). The choice of a forward model largely determines the total inversion time, and it is important to note that, even within a 1D formulation, it can take days or even weeks to invert a very large airborne dataset. Hence, we argue that a 1D forward formulation is still an important tool, and in many cases, the only viable solution for the inversion of very large airborne surveys. In this paper we present our latest development for speeding up this inversion process.

By far the most time-consuming operation in the inversion of TEM data is the calculation of the derivatives of the nonlinear forward modelling operator (Kirkegaard and Auken, 2015). For this reason, derivative estimations play an important role in the literature of geophysical data misfit minimisation (Huang and Palacky, 1991). Actually, minimising the time spent on derivative calculations is a general problem in inversion theory, which is not only limited to the solution of geophysical problems. Several different iterative minimisation algorithms are available, ranging from simple schemes that rely on computing a large number of low cost iterations, to more numerically costly algorithms with much better convergence properties. An example of the former is the conjugate gradient algorithm (Hestenes and Stiefel, 1952), which can be used to minimise a functional without any information on partial derivatives at all. On the other end of the spectrum we find the full Newton's method, which requires the calculation of both first and second order partial derivatives (i.e. the Jacobian and Hessian matrix). Generally, the computational balance favours the simple methods when derivatives are extremely numerically costly compared to the objective functional itself, whereas the Newton method becomes appealing when the opposite is true. Typically, the relative cost of derivative calculation and functional evaluation is found somewhere in between the extremes, making room for a range of quasi-Newton methods that implicitly approximate the second order derivatives. Such an algorithm is employed for the work presented here in the form of a Gauss-Newton method with the Levenberg-Marquardt modification (Marquardt, 1963). This method essentially represents a hybrid between simple gradient descent and the Gauss-Newton method, which requires the calculation of the full Jacobian matrix at each iteration. Comparable algorithms, such as the Broyden-Fletcher-Goldfarb-Shanno method (BFGS, see Romdhane et al. (2011) for a seismic application example), also approximate second order derivative information, but require only the objective function gradient to be computed in each iteration, rather than the full Jacobian matrix. This method can be attractive when it is more convenient to compute the gradient only, e.g. the adjoint state method (Plessix, 2006). For the case of the 1D TEM problem, however, the only benefit of the BFGS method is a reduction in memory consumption. Another popular choice is Broyden's update formula for the Jacobian matrix (Broyden, 1965, Loke and Barker, 1996; Torres-Verdín et al., 2000; Christiansen and Auken, 2004). This method eliminates the need for re-computing the Jacobian in every iteration of a quasi-Newton scheme, but often at a reduced convergence rate. Generally, it is desirable to use a minimisation method with as much first and second order information as possible (Haber et al., 2000), so rather than introducing more approximation in the minimisation algorithm, we choose to implement approximations in the derivative calculation itself. Oldenburg and Ellis (1991) used a similar approach by calculating 1D derivatives for inversion of 2D magnetotelluric data. Meanwhile, Christiansen and Auken (2004) performed 2D resistivity inversions using 1D derivatives, and Torres-Verdín et al. (2000) used a greatly simplified finite-difference grid for the derivative calculation.

In this paper, we investigate the performance benefits and applications of a specific hybrid implementation for airborne TEM data, relying on the Levenberg-Marquardt method for solving the inversion problem. The combined methodology is implemented in AarhusInv (Auken et al., 2014), and uses a full nonlinear forward model for the calculation of data misfit, and an approximate forward for the calculation of derivatives. Using this method we take much less computation time, while arriving at results that are virtually identical to those without the approximations. In this paper, we initially provide the theoretical background behind our method by describing our forward and inverse modelling schemes. We then present our results for hybrid inversion of both synthetic data and field data, after which we present our conclusions.

Forward modelling

For our hybrid inversion scheme, we use two distinct forward models: a full nonlinear 1D formulation for the evaluation of data misfit, and an approximate forward model for the calculation of partial derivatives for guiding the iterative steps of the inversion. The full nonlinear implementation follows the methodology of Ward and Hohmann (1988), whereas the approximate implementation uses an adaptive Born approximation (Christensen, 1997; Christensen et al., 2009). Both responses account for all effects of relevant acquisition system parameters, e.g. filters and waveforms (Christiansen et al., 2011).

In Figure 1, we show a comparison between the approximate and full nonlinear forward responses for a simulated SkyTEM system (Sørensen and Auken, 2004) at a characteristic instrument altitude of 30 m. The example in Figure 1*a* illustrates the most common case of very similar forward modelling results, whereas Figure 1*b* shows that significant deviations are also possible for specific models. In this latter case, we see individual gates varying ~20% when stated as late time apparent resistivity for a model with a deep lying conductor covered by a thick resistor. Based on the results of this figure it is clear that sizeable errors can be introduced if an inversion is performed solely on the approximate forward model. The results, however, are still so similar that the approximate forward model might prove a good choice for calculating partial derivatives; after all, partial derivatives are only needed for guiding the iterative steps of the inversion algorithm.

Inverse modelling

Inversion of TEM data is the process of determining the ground electrical resistivity distribution from the measurement of a decaying magnetic field. Thus, the resistivity distribution obtained by inversion is the subsurface resistivity model whose forward calculated response best matches the observed data. As the solution to this problem is, in general, ill-posed, it is convenient to impose additional requirements on the properties of the solution by including a regularising term. The general objective functional to minimise thus becomes:

$$\varphi(\mathbf{m}) = \|\mathbf{Q}_d\ (\mathbf{d}_{obs} - g(\mathbf{m}))\|_{L_2}^2 + \|\mathbf{Q}_p\ \mathbf{R}_p\ \mathbf{m}\|_{L_2}^2. \quad (1)$$

In this equation, the first term represents the squared L_2-distance between the weighted observed data $\mathbf{d}_{obs}$ and the forward response $g(\mathbf{m})$ of the model parameter vector $\mathbf{m}$. The second term, $\|\mathbf{Q}_p\mathbf{R}_p\mathbf{m}\|_{L_2}^2$, is a generic regularisation term that allows for including *a priori* information and/or smoothness constraints to the system of equations. $\mathbf{Q}_d$ and $\mathbf{Q}_p$ are the data and model weight matrices, respectively. For our purposes we set $\mathbf{Q}_d$ to be a diagonal matrix holding the inverse of the data variances, and use $\mathbf{Q}_p$ to specify the different degrees of variability associated with spatial constraints as described by $\mathbf{R}_p$. For full details on our use of spatial regularisation constraints see the papers on laterally constrained inversion (LCI) and spatially constrained inversion (SCI) (Auken and Christiansen, 2004; Viezzoli et al., 2008).

The framework of our implementation is the AarhusInv code (Auken et al., 2014), which manages the minimisation of the nonlinear objective functional of Equation 1 using the iterative Levenberg-Marquart minimisation algorithm. The algorithm provides an iterative model update formula for the (n+1)-th iteration:

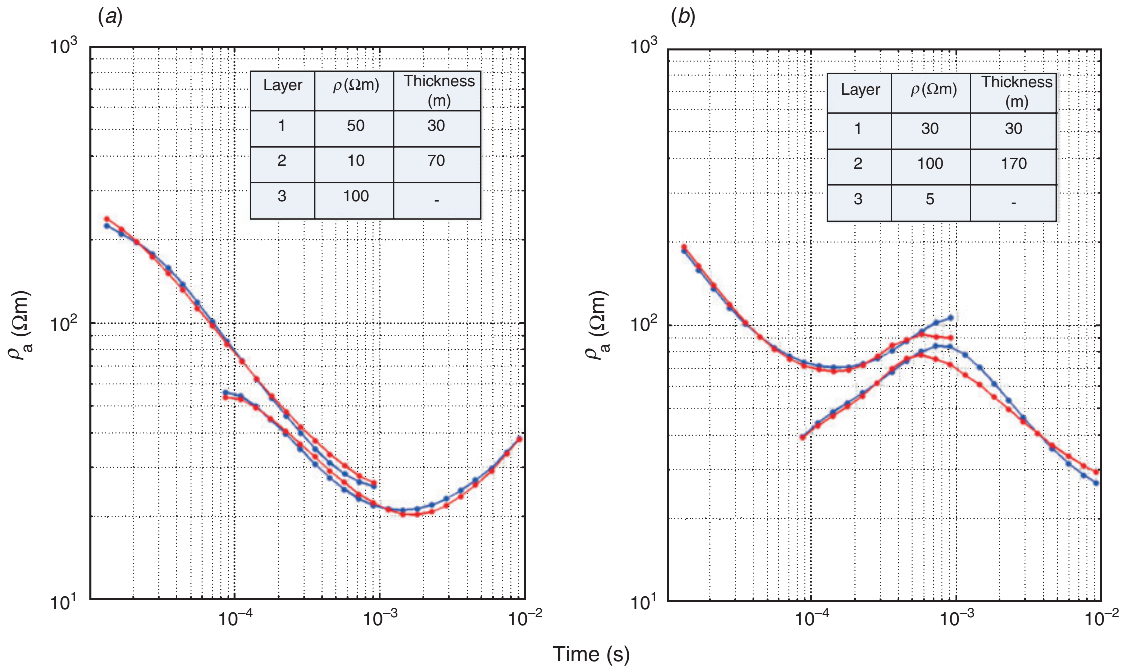

Fig. 1. Forward modelling examples for two distinct models using the characteristics of the dual moment SkyTEM system configuration at an altitude of 30 m. Model (*a*) has a shallow resistive last layer, while model (*b*) has a deep conductive last layer. The blue and red lines show responses based on the full nonlinear forward model and the approximate forward model, respectively.

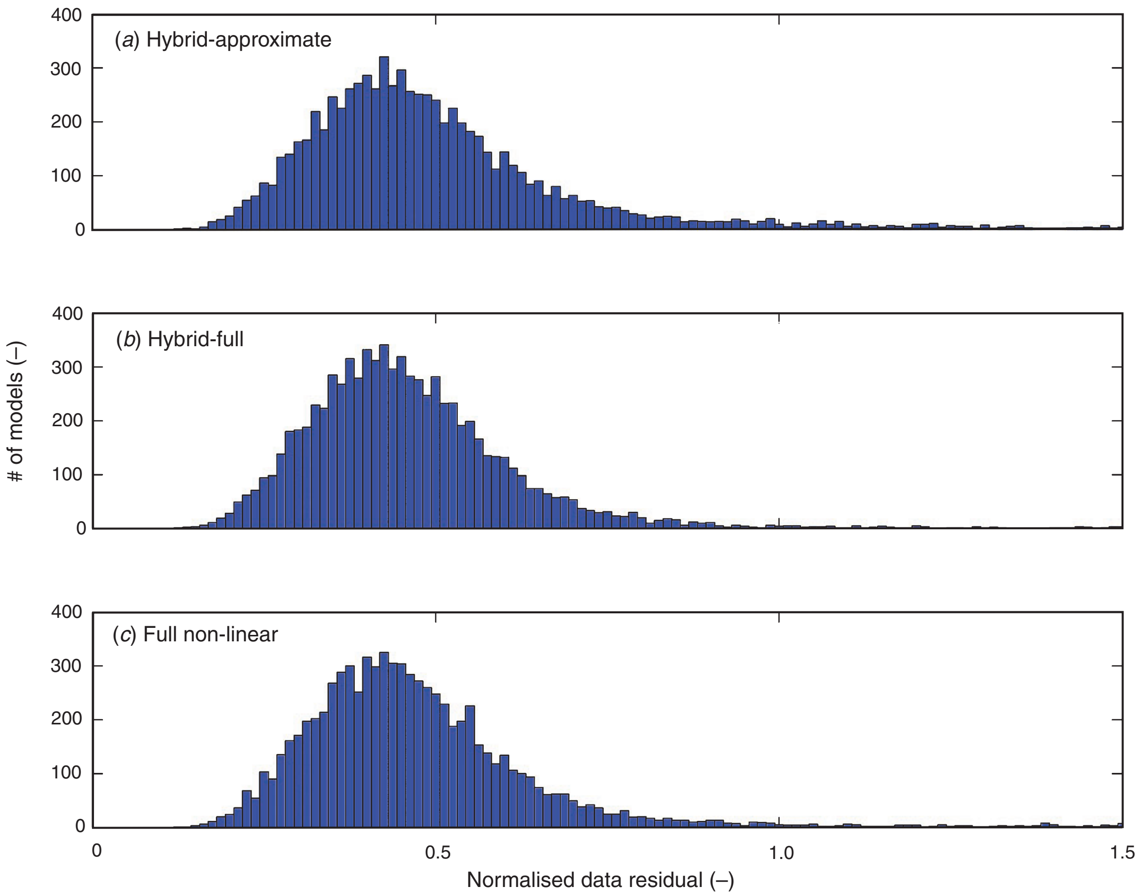

Fig. 2. Data fit distributions for inversions of the same synthetic dataset, calculated from 8000 randomly generated models and perturbed by realistic noise. All sub-plots are based on inversions using the same methodology and settings, except for the degree of approximation used for calculating the partial derivatives of the Jacobian matrix. (*a*) The Jacobian is calculated from the approximate forward model in every iteration. (*b*) The Jacobian is calculated from the approximate forward model for most iterations, but finalised with a few iterations of full nonlinear derivatives. (*c*) The Jacobian is calculated from full nonlinear forward model in every iteration (reference inversion).

$$\mathbf{m}_{n+1} = \mathbf{m}_n + [\mathbf{G}_n^T \mathbf{C}_{obs}^{-1} \mathbf{G}_n + \mathbf{R}_p^T \mathbf{C}_c^{-1} \mathbf{R}_p + \lambda \mathbf{I}]^{-1} \cdot [\mathbf{G}_n^T \mathbf{C}_{obs}^{-1} (\mathbf{d}_{obs} - g(\mathbf{m}_n)) + \mathbf{R}_p^T \mathbf{C}_c^{-1} (-\mathbf{R}_p \mathbf{m}_n)] \quad (2)$$

Here, $\mathbf{G}_n$ is the Jacobian matrix based on the n-th model, $\mathbf{I}$ is the identity matrix, $\mathbf{C}_{obs}^{-1} = \mathbf{Q}_d^T \mathbf{Q}_d$ is a covariance matrix specifying the data uncertainties as described above, while $\mathbf{C}_c^{-1} = \mathbf{Q}_p^T \mathbf{Q}_p$ specifies the strength of the regularising constraints. λ is a Marquardt damping parameter that is iteratively updated over the course of the inversion to stabilise and improve the performance of the minimisation process (Marquardt, 1963). Roughly speaking, one can say that the first term of the first bracket expresses the direction and size of the step as suggested by the data and data errors; the second term expresses the direction as suggested by the constraints (roughness). In the second bracket, the first term balances the direction according to the misfit with the observed data, and the second term balances the step with the misfit to the suggested constraints.

For the purposes of this paper we compare three iterative inversion processes, (A)–(C), differing only in their calculation of the elements of $\mathbf{G}_n$. All approaches use a standard first order finite difference formula for calculating partial derivatives from two forward calculations separated by a small perturbation. Methods (A) and (B) are fast hybrid methods utilising the approximate forward model for the calculation of $\mathbf{G}_n$, whereas method (C) is a slower reference inversion utilising the full nonlinear forward model for all derivative calculations. For method (A) we use the highest degree of approximation in the sense that we always use the Born approximate forward model for calculating the derivatives. Method (B), on the other hand, uses the approximate forward model for all iterations until the convergence criteria are met. At this stage, the algorithm shifts to calculating the derivatives using the full nonlinear forward model for at least one more iteration, but typically 2–3 iterations, in order to handle the potential situation of being caught in a local minimum.

Inversion of synthetic data

In order to ensure a comprehensive comparison of our three different inversion strategies, we now compare the accuracy in both data and model space. To do this, we randomly generated 8000 models of five layers. These random models are characterised by layer resistivity values and thicknesses uniformly distributed in the interval 2–200 Ωm and 5–50 m, respectively. These synthetic models were turned into synthetic SkyTEM soundings (Sørensen and Auken, 2004) using the full nonlinear forward model described in the forward modelling section, and perturbed by synthetic noise. To make the soundings resemble actual field data, we added two distinct noise contributions: a uniform Gaussian component with 5%

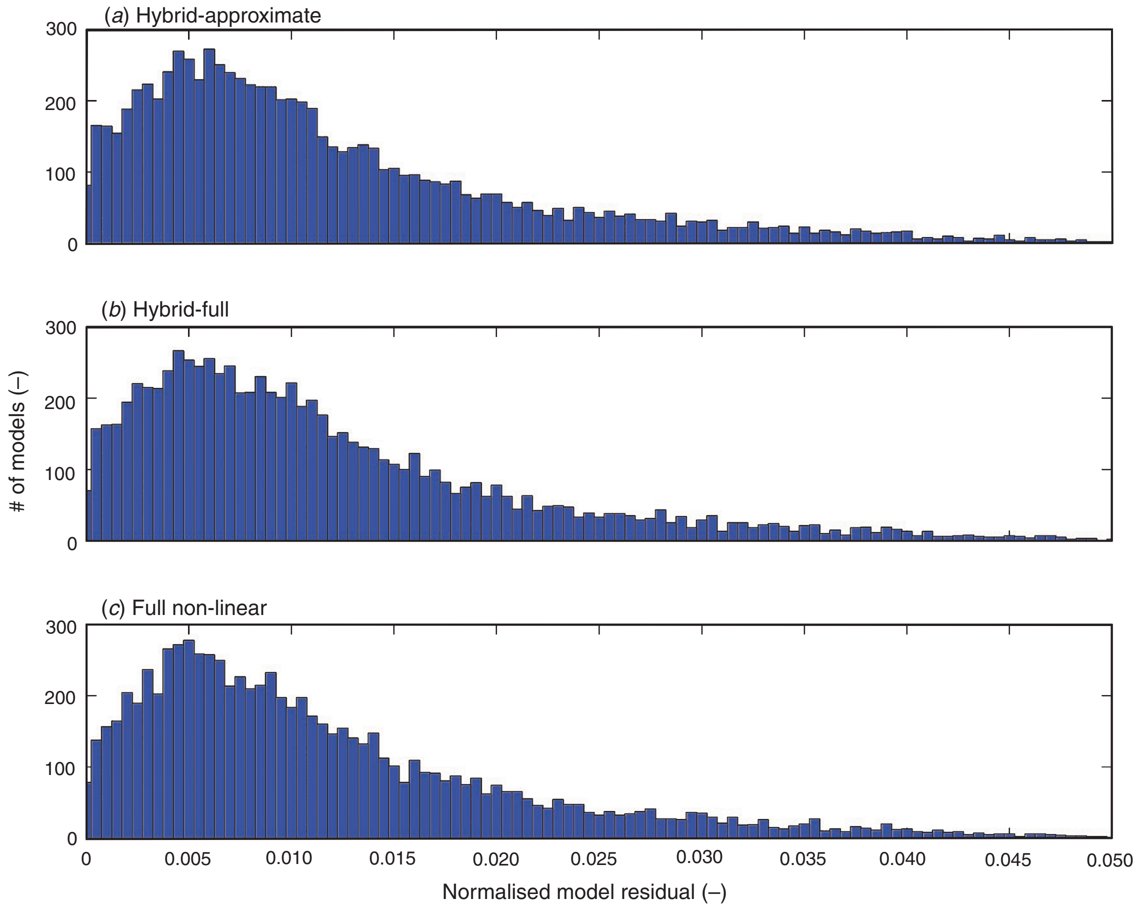

Fig. 3. Model fit distributions for inversions of the same synthetic dataset, calculated from 8000 randomly generated models and perturbed by realistic noise. All sub-plots are based on inversions using the same methodology and settings, except for the degree of approximation used for calculating the partial derivatives of the Jacobian matrix. (*a*) The Jacobian is calculated from the approximate forward model in every iteration. (*b*) The Jacobian is calculated from the approximate forward model for most iterations, but finalised with a few iterations of full nonlinear derivatives. (*c*) The Jacobian is calculated from full nonlinear forward model in every iteration (reference inversion).

standard deviation and a time-dependent contribution falling off as $t^{-1/2}$ with a value of 5 nV/m^2 at 1 ms (Auken et al., 2008).

In Figure 2, we show the data residual distributions for the results of the three different inversion types, differing only in the degree of approximation used for the calculation of the Jacobian matrix $\mathbf{G}_n$. All inversions were performed using the same settings for obtaining 20-layer 1D models of fixed layer boundaries using vertical smoothing regularisation. The data fits come out very similar for the three different inversion types. Generally, data misfits are below 1 due to a uniform contribution in our noise model following the same approach as Kirkegaard et al. (2012). In Figure 3, we show an almost identical figure, but this time we compare the residual in model space for each inversion type. The residual between the true 5-layer model and each reconstructed 20-layer model was calculated by resampling them to obtain two directly comparable 300-layer models. With the dense reparameterisation, the error due to the differences in original discretisation becomes negligible. After the resampling, the normalised model residual can be calculated in the standard way as the root mean square:

$$\Delta\mathbf{m} = \sqrt{\frac{1}{300}\sum_{i=1}^{300}\left(\frac{m_i^{(true)} - m_i^{(inv.)}}{m_i^{(true)}}\right)^2}. \quad (3)$$

By comparing the results of the hybrid inversions (Figure 3*a*, *b*) with the full nonlinear result of Figure 3*c*, it is clear that the different inversion schemes show almost equally good performance in the model's space. In order to further quantify the model space differences, we should note that the mean of all the three normalised model residual distributions is 0.012, while their corresponding standard deviations are 0.013 (Figure 3*a*), 0.010 (Figure 3*b*) and 0.010 (Figure 3*c*). Hence, the differences of the mean values are largely within the standard deviation intervals. A similar argument is also true for the data misfit distributions.

All the examples above are performed on a strictly 1D model. We expect the behaviour to be the same for any 2D or 3D affected model that can be reasonably well inverted using a 1D model assumption with the full nonlinear forward. If the full nonlinear inversion cannot find a reasonable model describing the data, the hybrid solutions will also fail.

Having investigated the data and model space properties of the hybrid inversion schemes, we then compare the performance of the algorithms, as seen in Figure 4. In Figure 4*a* we show the distribution of speed-up factors for the models in the synthetic dataset compared to the time consumption of the reference inversion (C). For the most approximate method (A), we find an average speed-up factor of 6.5, whereas the speed-up factor for the less approximate (B) scheme is 2.8. It is worth mentioning that the number of iterations used to solve the inversion problem increases slightly for the hybrid (B) strategy because it calculates iterations with accurate derivatives where method (A) stops. In particular, Figure 4*b* shows that the number of iterations required for the hybrid scheme (A) remains, on average, unchanged with respect to the iterations necessary for the full nonlinear scheme (C), while the hybrid (B) strategy needs 2–3 more iterations.

Inversion of field data

Having assessed the accuracy and performance of the hybrid inversion schemes on synthetic data, we proceed to applying the three inversion algorithms to actual field data. Our field example consists of a portion of a larger SkyTEM dataset collected within the CLIWAT project framework (Harbo et al., 2011) in the western part of the Danish-German border area. Specifically,

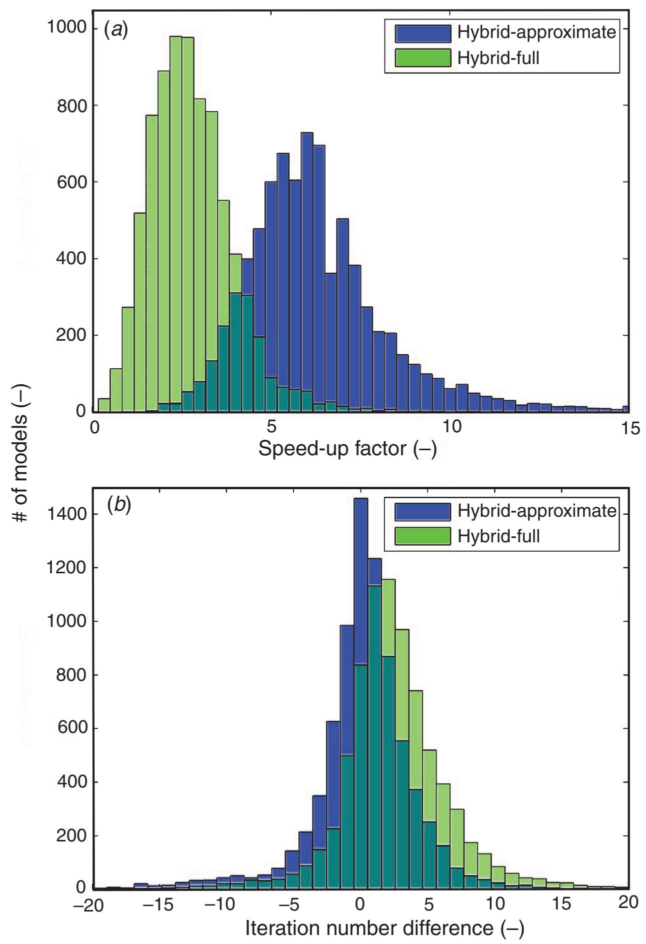

Fig. 4. Performance of the hybrid inversion schemes. (*a*) Speed-up factor with respect of the full nonlinear inversion. (*b*) Difference in the number of iterations with respect to the full nonlinear inversion.

we focus on the data subset recorded in the survey carried out on the German side, close to Niebüll, during September 2008. The survey is presented and analysed in detail by Jørgensen et al. (2012). We chose this dataset because it includes areas of mild and large resistivity contrasts.

Figure 5 shows west-east cross-sections of the inversion results for a flight line inverted for the three distinct inversion types (A)–(C). The data was inverted for 1D models of 29 layers, utilising vertical and lateral smoothness constraints through the spatially constrained inversion (SCI) methodology (Viezzoli et al., 2008). Each cross-section in Figure 5 includes a data residual curve shown in black. The inversion results are blanked below the depth of investigation (Christiansen and Auken, 2012). When inspecting the figure, we can distinguish two parts. The first part between profile coordinates 0–5500 m is very heterogeneous, appears more resistive and is crossed by several elongated, lower resistive bodies. This appearance can be explained by a strong influence from glacial processes. The second part (profile coordinates 5500–14000 m) consists of a less heterogeneous sequence with roughly plane-parallel layering and a clear low-resistive body. This part is primarily Miocene layers that are undisturbed by glacial processes.

From the comparison of the inversions in Figure 5*a*–*c*, it is clear that all the three inversion results are close to being identical; to identify them takes a much more detailed display than possible here. Likewise, it is very hard to detect any differences between the data residual curves among the (A)–(C) cases in Figure 5.

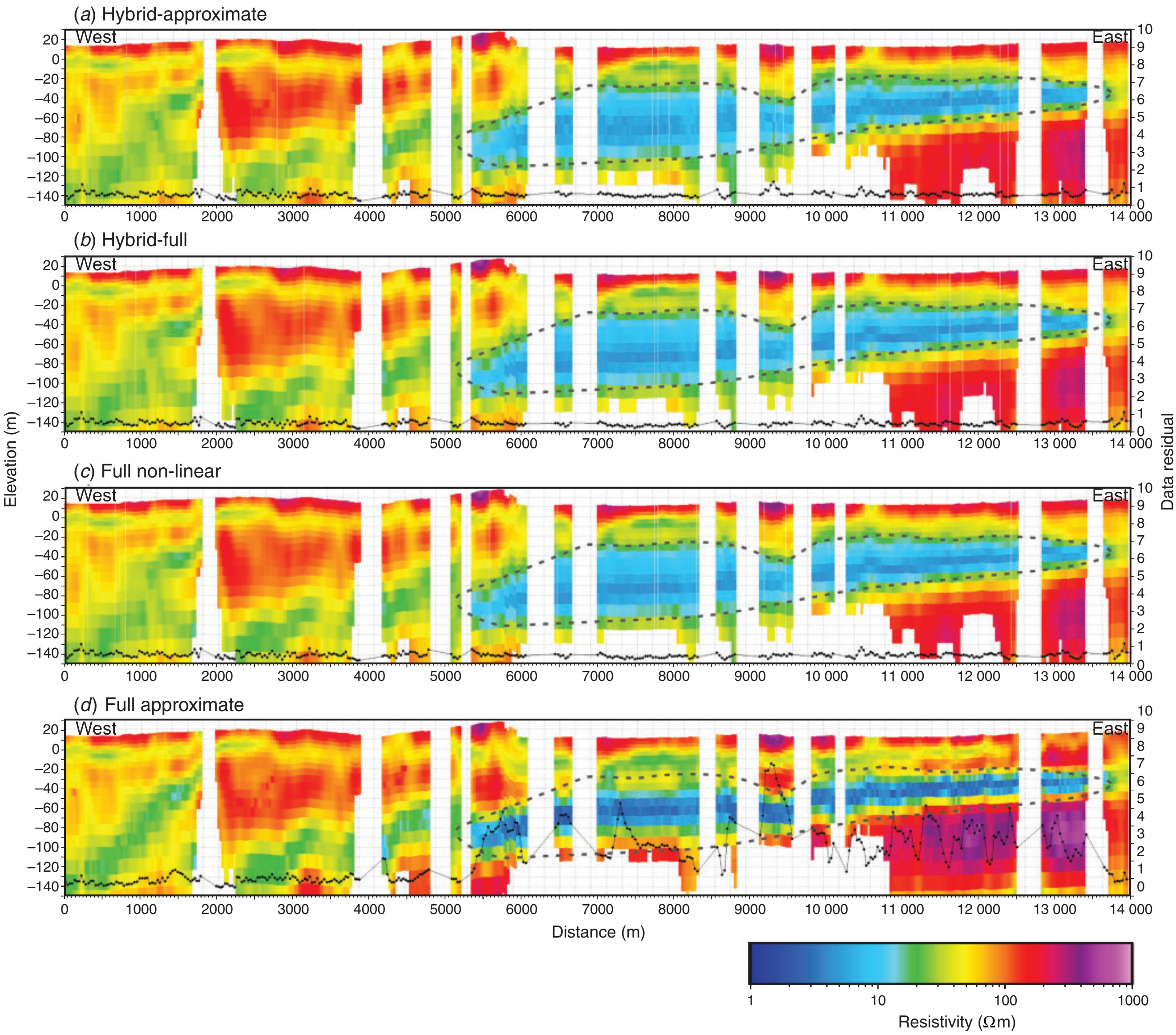

Fig. 5. Example inversion results for field dataset with data residuals plotted as black line. The results are blanked below the depth of investigation. (*a*) The Jacobian is calculated from the approximate forward model in every iteration. (*b*) The Jacobian is calculated from the approximate forward model for most iterations, but finalised with a few iterations of full nonlinear derivatives. (*c*) The Jacobian is calculated from full nonlinear forward model in every iteration (reference inversion). (*d*) The Jacobian and forward model are both calculated by using the Born approximation.

Having assessed the inversion results from cases (A)–(C), we included another approximation (D) (Figure 5*d*) to further illustrate potentially misleading results based on a full Born approximation imaging. In case (D), instead of using a full nonlinear forward response as in (A)–(C), the objective functional is evaluated by using a Born approximation forward model. Note, however, that the data residuals shown are computed using the accurate forward response to reflect the actual misfit, rather than the misfit obtained by the approximate modelling itself when the convergence criteria is met. For example, by comparing Figure 5*c* and Figure 5*d*, it is seen that the reconstructions of the first left part of the sections are nearly identical, both in terms of model results and data fit, with a slight favour to the accurate response in (C). This is not surprising, as this portion of the section is characterised by low resistivity contrasts, and the Born approximation is known to perform well in the presence of relatively small conductivity variations (Christensen, 1997). This is confirmed by the fact that in the right part of the profile, where resistivity contrasts are higher, the data fits of the approximate algorithm (D) are significantly worse. The models also differ significantly in the right part of the profiles with the thickness of the conductive body (dash outline) being underestimated by up to 50 m (e.g. around coordinate 7600 m). Around coordinate 11 000–12 500 m, a very different layer sequence is suggested in the full approximate model (D), which is most likely explained by effects similar to what was discussed for Figure 1.

Conclusion

We have presented the theoretical background and computational motivation for investigating a hybrid inversion scheme for airborne TEM data that introduces approximations only in the calculation of partial derivatives. The objective function itself is evaluated with a full nonlinear 1D forward model, whereas derivatives are calculated from an adaptive Born approximation. Introducing approximation only in the calculation of derivatives leaves the physical description of the system unaltered, thus providing potential for a significant inversion speed up with very little loss of accuracy. This hypothesis is investigated by comparing three different inversion methodologies, differing only in their calculating of the partial derivatives: (A) the Jacobian is calculated from an approximate forward model in every iteration; (B) the Jacobian is calculated from an approximate forward model for most iterations, but finalised with a few iterations using full nonlinear derivatives; and (C) the Jacobian is calculated from a full nonlinear forward model in every iteration (reference inversion). The accuracy of the three inversion methodologies was tested on a large set of synthetic data, with the conclusion that the results are virtually identical in both model and data space. With respect to performance, we find that method (A) provides an average speed-up factor of around 7 with a corresponding value of 3 for method (B). We back up our synthetic inversion comparison by also inverting a relevant field dataset, and find that the performance results agree with those from the synthetic case. We conclude that our hybrid inversion scheme provides a very efficient means for speeding up the inversion of airborne TEM data, using different degrees of approximation to match the application at hand. Method (A) provides by far the greatest speed up at the expensive of only a few minor deviations from the reference result. We therefore conclude that this approach can be used for any application that can tolerate a small amount of inaccuracy, or for any preliminary inversion job. Method (B) provides a smaller speed up, which is compensated by the fact this it produces models that can be considered identical to those of the reference inversion. We thus conclude that this method can safely be used to speed up the inversion of any airborne TEM dataset, as it provides absolute negligible loss of accuracy.

Acknowledgments

We thank Niels Bøie Christensen for his invaluable contributions to the project and Andrea Viezzoli from Aarhus Geophysics ApS for his useful suggestions and comments. We further acknowledge HOBE, the Villum Centre of Excellence, for their partial funding.

References

Allard, M., 2007, On the origin of the HTEM species, *in* B. Milkereit, ed., *Proceedings of Exploration 07: Fifth Decennial International Conference on Mineral Exploration*: Decennial Mineral Exploration Conferences, 355–374.

Auken, E., and Christiansen, A. V., 2004, Layered and laterally constrained 2D inversion of resistivity data: *Geophysics*, **69**, 752–761. doi:10.1190/1.1759461

Auken, E., Christiansen, A. V., Jacobsen, L., and Sørensen, K. I., 2008, A resolution study of buried valleys using laterally constrained inversion of TEM data: *Journal of Applied Geophysics*, **65**, 10–20. doi:10.1016/j.jappgeo.2008.03.003

Auken, E., Christiansen, A. V., Kirkegaard, C., Fiandaca, G., Schamper, C., Behroozmand, A. A., Binley, A., Nielsen, E., Effersø, F., Christensen, N. B., Sørensen, K. I., Foged, N., and Vignoli, G., 2014, An overview of a highly versatile forward and stable inverse algorithm for airborne, ground-based and borehole electromagnetic and electric data: *Exploration Geophysics*, doi:10.1071/EG13097

Broyden, C. G., 1965, A class of methods for solving nonlinear simultaneous equations: *Mathematics of Computation*, **19**, 577–593. doi:10.1090/S0025-5718-1965-0198670-6

Christensen, N. B., 1997, Electromagnetic subsurface imaging. A case for adaptive Born approximation: *Surveys in Geophysics*, **18**, 477–510. doi:10.1023/A:1006593408478

Christensen, N. B., Reid, J. E., and Halkjaer, M., 2009, Fast, laterally smooth inversion of airborne time-domain electromagnetic data: *Near Surface Geophysics*, **7**, 599–612. doi:10.3997/1873-0604.2009047

Christiansen, A. V., and Auken, E., 2004, Optimizing a layered and laterally constrained 2D inversion of resistivity data using Broyden's update and 1D derivatives: *Journal of Applied Geophysics*, **56**, 247–261. doi:10.1016/S0926-9851(04)00055-2

Christiansen, A. V., and Auken, E., 2012, A global measure for depth of investigation: *Geophysics*, **77**, WB171–WB177. doi:10.1190/geo2011-0393.1

Christiansen, A. V., Auken, E., and Viezzoli, A., 2011, Quantification of modeling errors in airborne TEM caused by inaccurate system description: *Geophysics*, **76**, F43–F52. doi:10.1190/1.3511354

Cox, L. H., Wilson, G. A., and Zhdanov, M. S., 2010, 3D inversion of airborne electromagnetic data using a moving footprint: *Exploration Geophysics*, **41**, 250–259. doi:10.1071/EG10003

Haber, E., Ascher, U. M., and Oldenburg, D., 2000, On optimization techniques for solving nonlinear inverse problems: *Inverse Problems*, **16**, 1263–1280. doi:10.1088/0266-5611/16/5/309

Harbo, M. S., Pedersen, J., Johnsen, R., and Petersen, K., eds., 2011, *Groundwater in a future climate*: Danish Ministry of the Environment Nature Agency.

Hestenes, M. R., and Stiefel, E., 1952, Methods of conjugate gradients for solving linear systems: *Journal of Research of the National Bureau of Standards*, **49**, 409–436. doi:10.6028/jres.049.044

Huang, H., and Fraser, D. C., 1996, The differential parameter method for multifrequency airborne resistivity mapping: *Geophysics*, **61**, 100–109. doi:10.1190/1.1574674

Huang, H., and Palacky, G. J., 1991, Damped least-squares inversion of time-domain airborne EM data based on singular value decomposition: *Geophysical Prospecting*, **39**, 827–844. doi:10.1111/j.1365-2478.1991.tb00346.x

Jørgensen, F., Scheer, W., Thomsen, S., Sonnenborg, T. O., Hinsby, K., Wiederhold, H., Schamper, C., Roth, B., Kirsch, R., and Auken, E., 2012, Transboundary geophysical mapping of geological elements and salinity distribution critical for the assessment of future sea water intrusion in response to sea level rise: *Hydrology and Earth System Sciences*, **16**, 1845–1862. doi:10.5194/hess-16-1845-2012

Kirkegaard, C., and Auken, E., 2015, A parallel, scalable and memory efficient inversion code for very large scale airborne EM surveys: *Geophysical Prospecting*, **63**, 495–507. doi:10.1111/1365-2478.12200

Kirkegaard, C., Sonnenborg, T. O., Auken, E., and Flemming, J., 2011, Salinity distribution in heterogeneous coastal aquifers mapped by airborne electromagnetics: *Vadose Zone Journal*, **10**, 125–135. doi:10.2136/vzj2010.0038

Kirkegaard, C., Foged, N., Auken, E., Christiansen, A. V., and Sørensen, K. I., 2012, On the value of including x-component data in 1D modeling of electromagnetic data from helicopterborne time domain systems in horizontally layered environments: *Journal of Applied Geophysics*, **84**, 61–69. doi:10.1016/j.jappgeo.2012.06.006

Legault, J. M., Witter, J. B., Berardelli, P., Lombardo, S., and Orta, M., 2011, Recent ZTEM airborne AFMAG EM survey results over Reese River and other geothermal test areas: Geothermal Resources Council 2011 Annual Meeting, 23–26 October 2011, San Diego, California, **35**, 879–884.

Ley-Cooper, A. Y., Viezzoli, A., Guillemoteau, J., Vignoli, G., Macnae, J., Cox, L., and Munday, T., 2015, Airborne electromagnetic modelling options and their consequences in target definition: *Exploration Geophysics*, **46**, 74–84. doi:10.1071/EG14045

Loke, M. H., and Barker, R. D., 1996, Rapid least squares inversion of apparent resistivity pseudosections by a quasi-Newton method: *Geophysical Prospecting*, **44**, 131–152. doi:10.1111/j.1365-2478.1996.tb00142.x

Macnae, J., King, A., Stolz, N., Osmakoff, A., and Blaha, A., 1998, Fast AEM data processing and inversion: *Exploration Geophysics*, **29**, 163–169. doi:10.1071/EG998163

Marquardt, D., 1963, An algorithm for least squares estimation of nonlinear parameters: *SIAM Journal on Applied Mathematics*, **11**, 431–441. doi:10.1137/0111030

Minsley, B., Cox, L. H., Brodie, R., Wilson, G. A., Abraham, J. D., and Zhdanov, M. S., 2012, A comparison of AEM inversion methods for discontinuous permafrost at Fort Yukon, Alaska: Symposium on the Application of Geophysics to Environmental and Engineering Problems, SAGEEP, Tuscon, Arizona.

Oldenburg, D. W., and Ellis, R. G., 1991, Inversion of geophysical data using an approximate inverse mapping: *Geophysical Journal International*, **105**, 325–353. doi:10.1111/j.1365-246X.1991.tb06717.x

Pfaffhuber, A. A., Monstad, S., and Rudd, J., 2009, Airborne electromagnetic hydrocarbon mapping in Mozambique: *Exploration Geophysics*, **40**, 237–245. doi:10.1071/EG09011

Plessix, R. E., 2006, A review of the adjoint-state method for computing the gradient of a functional with geophysical applications: *Geophysical Journal International*, **167**, 495–503. doi:10.1111/j.1365-246X.2006.02978.x

Romdhane, A., Grandjean, G., Brossier, R. M., Rejiba, F., Operto, S., and Vineux, J., 2011, Shallow structure characterization by 2D elastic full-waveform inversion: *Geophysics*, **76**, R81–R93. doi:10.1190/1.3569798

Sengpiel, K. P., and Siemon, B., 2000, Advanced inversion methods for airborne electromagnetic exploration: *Geophysics*, **65**, 1983–1992. doi:10.1190/1.1444882

Siemon, B, Christiansen, A. V., and Auken, E, 2009, A review of helicopter-borne electromagnetic methods for groundwater exploration: *Near Surface Geophysics*, **7**, 629–646.

Sørensen, K. I., and Auken, E., 2004, SkyTEM – a new high-resolution helicopter transient electromagnetic system: *Exploration Geophysics*, **35**, 191–199.

Torres-Verdín, C., Druskin, V. L., Fang, S., Knizhnerman, L. A., and Malinverno, A., 2000, A dual-grid nonlinear inversion technique with applications to the interpretation of dc resistivity data: *Geophysics*, **65**, 1733–1745. doi:10.1190/1.1444858

Viezzoli, A., Christiansen, A. V., Auken, E., and Sørensen, K. I., 2008, Quasi-3D modeling of airborne TEM data by spatially constrained inversion: *Geophysics*, **73**, F105–F113. doi:10.1190/1.2895521

Viezzoli, A., Munday, T., Auken, E., and Christiansen, A. V., 2010, Accurate quasi 3D versus practical full 3D inversion of AEM data – the Bookpurnong case study: *Preview*, **149**, 23–31.

Ward, S. H., and Hohmann, G. W., 1988, Electromagnetic theory for geophysical applications, *in* M. N. Nabighian, ed., *Electromagnetic methods in applied geophysics*: Society of Exploration Geophysicists (SEG), 131–311.

Wilson, G. A., Raiche, A., and Sugeng, F., 2006, 2.5D inversion of airborne electromagnetic data: *Exploration Geophysics*, **37**, 363–371.

Zhdanov, M. S., 2002, *Geophysical inverse theory and regularization problems*: Elsevier.